JOURNAL OF AGRICULTURAL AND FOOD CHEMISTRY
ARTICLE

J. Agric. Food Chem. 2010, 58, 11695–11702 11695
DOI:10.1021/jf102944c

Selective Delivery of Cargo Entities to Tumor Cells by Nanoscale Artificial Oil Bodies

Chung-Jen Chiang,*,† Chih-Jung Chen,† Li-Jen Lin,‡ Chih-Hsiang Chang,§ and Yun-Peng Chao*,§

†Department of Medical Laboratory Science and Biotechnology, China Medical University, Taichung, Taiwan, ‡School of Chinese Medicine, China Medical University, Taichung, Taiwan, and §Department of Chemical Engineering, Feng Chia University, Taichung, Taiwan

Artificial oil bodies (AOBs) are oil droplets that result from self-assembly of a mixture containing triacylglycerols, phospholipids, and membrane proteins of plant seeds. Owing to their small size, stability, hydrophobic core, biocompatibility, and biodegradability, AOBs were explored to examine their feasibility as a drug delivery carrier. This was approached by fusion sesame oleosin (Ole), the primary membrane protein of seed oil bodies, with a small domain consisting of the arginine-glycine-aspartic acid (RGD) motif. The resulting Ole-RGD fusion protein was overproduced in *Escherichia coli* and then isolated for reconstitution of AOBs. At the optimal condition, the size of stable AOBs was within the range of 100−400 nm. Furthermore, AOBs entrapped with a hydrophobic fluorescence dye were incubated with human tumor cells. As visualized by fluorescent microscopy and confocal microscopy, the RGD-tagged AOBs were able to selectively target cells expressing the $\alpha_v\beta_3$ integrin. Moreover, these AOBs were effectively internalized and the fluorescence dye that they carried was subsequently released inside the cells. The percentage of cells internalized by AOBs could reach 80% as analyzed by flow cytometry. Taken together, it illustrates a great promise of this proposed approach for targeted delivery of cargo entities to tumor cells.

KEYWORDS: Oil body; oleosin; tumor targeting; drug delivery; RGD

INTRODUCTION

Oil bodies are small spherical vacuoles that appear within the cells of plant seeds. They are composed of triacylglycerols (TAGs) surrounded by a monolayer of phospholipids (PLs) and provide the fuel needed for seedling growth during seed germination(*1*,*2*). With the entrapment of membrane proteins into PLs, oil bodies have the size of 0.5−2 μm in diameter on average and exhibit remarkable stability in the form of separate entities both *in vivo* and *in vitro*. This stability has been attributed to the steric hindrance and electronegative repulsion contributed by oleosin (Ole), known as the primary membrane protein in oil bodies (*3*). The structure of Ole consists of the central hydrophobic region linked with two peptide arms. The central region is embedded into the TAG matrix while two terminal domains of the negative charge are extruded from the surface of oil bodies (*4*).

Reconstitution of oil bodies *in vitro*, called artificial oil bodies (AOBs), is technically feasible. This is carried out by mixing three essential constituents including TAGs (94−98%), PLs (0.5−2%), and membrane proteins (0.5−3.5%) (*5*,*6*). In addition to thermal and structural stability, the size of AOBs can be modulated by varying the ratio of their constituents and, particularly, correlates with the amount of membrane proteins in use (*7*). Formed by Ole that is expressed in *Escherichia coli*, AOBs have been shown to be comparable in size, topology, and stability with those encapsulated with native Ole isolated from seed oil bodies (*8*). Owing to its unique structural and topological features, Ole has been utilized to formulate AOBs for many biotechnological applications by our research group. These practices include the scaffold-assisted refolding and purification of recombinant proteins (*9*−*11*), one-step immobilization of enzymes (*12*), and encapsulation of probiotics for oral administration (*13*).

Therapeutic application of hydrophobic agents still faces challenges. Owing to their poor solubility, hydrophobic drugs administrated orally or intravenously result in many problems, usually leading to, for instance, low bioavailability and high local concentration at the site of aggregate deposition (*14*, *15*). This issue has been addressed by development of various drug carrier systems, such as liposome (*16*), synthetic polymers (*17*), micelles (*18*), and many others (*19*). These systems are aimed at increasing the drug bioavailability in the pathological area in the hope of protecting normal tissues from undesirable side effects. Although some promising results are reported, many technical difficulties remain to be overcome (*20*).

The prerequisites for a drug carrier include small size, biocompatibility, and biodegradability. AOBs appear to possess these characteristics. They comprise natural lipids as well as proteins and have a size of nanoscale. Particularly, their hydrophobic core is appealing for the entrapment of water-repelling agents. Therefore, this study was initiated to explore the feasibility of AOBs as a drug delivery vehicle. As an initial attempt, Ole was fused with a small

*Corresponding authors. C.-J.C.: tel, 886-4-22003366 ext 7227; fax, 886-4-22057414; e-mail, cjchiang@mail.cmu.edu.tw. Y.-P.C.: tel, 886-4-24517250 ext 3677; fax, 886-4-24510890; e-mail, ypchao@fcu.edu.tw.

Published on Web 10/22/2010

peptide containing the core sequence of arginine-glycine-aspartic acid (RGD) to its C terminus. The RGD-based ligand is known to specifically interact with $\alpha_v\beta_3$ integrin of human tumor cells (*21*). After expressing in *E. coli*, this hybrid protein (Ole-RGD) was recovered to constitute AOBs. Followed by entrapment of a hydrophobic fluorescence dye, AOBs tagged with RGD could be selectively and effectively internalized by $\alpha_v\beta_3$ integrin-positive cells. Subsequently, the fluorescence dye was freely released into cells. This is the first report that illustrates a great potential of AOBs for targeted delivery of hydrophobic agents to tumor cells.

MATERIALS AND METHODS

DNA Manipulation. Plasmid pJO1-Ole-TR contains the RGD domain (GGCRGDMFGC) fused to the C terminus of Ole. It was constructed by introduction of the RGD motif into downstream of Ole on plasmid pJO1-Ole using polymerase chain reaction (PCR). Plasmid pJO1-Ole was previously constructed to carry the Ole gene under the control of the T7 promoter (*10*). With primer JO21 (attgatccgaattaattccgatatc) and JO22 (attggatccggcggctgccgcggcgatatgtttggctgctaagcttgcggccgcactcgagcac), the whole plasmid DNA with an extension containing the RGD motif was synthesized by PCR. The resulting PCR DNA was digested with *Bam*HI and then self-ligated to obtain plasmid pJO1-Ole-TR. Finally, the correctness of the plasmid construct was confirmed by DNA sequencing.

Analyses of Protein Overproduction. Plasmid pJO1-Ole-TR and pJO1-Ole were transformed into *E. coli* strain BL21 (DE3) (Novagen) to produce strain BL21-OleTR and BL21-Ole, respectively. Bacterial growth was monitored for their growth by turbidimetrical measurement at 550 nm (OD_{550}). One unit at OD_{550} corresponds to 1.8×10^8 cells per mL. With the initial cell density of 0.1 at OD_{550}, two recombinant strains were cultivated in shake flasks containing Luria−Bertani (LB) medium(*22*) at 37 °C. Bacterial cultures were induced with 100 μM IPTG for protein overproduction upon reaching 0.5 at OD_{550}. Four hours later, bacteria were harvested by centrifugation and resuspended in 1 mL of 0.01 M sodium phosphate buffer (pH 7.5). As reported previously (*23*), proteins were analyzed by dodecyl sulfate−polyacrylamide gel electrophoresis (SDS−PAGE). To perform SDS−PAGE analyses, harvested bacteria were lysed by sonication. After centrifugation, the supernatant and the pellet were resolved onto 8% polyacrylamide gel and stained with Coomassie blue R-250 for observation.

Reconstitution of Fluorescent AOBs. AOBs were reconstituted essentially following the previous method (*10*). In essence, the density of bacteria as harvested was adjusted to reach 10 at OD_{550} using 0.01 M sodium phosphate buffer (pH 7.5). Bacteria were then disrupted by French press and fractioned into the supernatant and pellet part by centrifugation. Unless stated otherwise, AOBs were prepared by mixing 100 μg of plant oils, 150 μg of PL, and 100 μg of Ole-RGD in 1 mL of 10 mM sodium phosphate buffer (pH 7.5). Fluorescent AOBs were formed in the same way except that 1 μg of yellow GGK dye (Widetex Co., Taiwan) was additionally added. The plant oil selected for use was soybean oil (Taiwan Sugar Co., Taiwan), canola oil (Leader Price Co., Taiwan), vegetable oil (Taisun Co., Taiwan), sunflower oil (Leader Price Co., Taiwan), olive oil (Taisun Co., Taiwan), and mineral oil (Sigma, USA). The mixture was subjected to sonication three times on ice with the amplitude set at 20% and 10 s. Subsequently, AOBs were removed from the top after centrifugation. Followed by washing, AOBs were stored in the buffer solution until use.

Analyses of AOBs' Morphology, Size, and Stability. The morphology of AOBs prepared at various conditions was analyzed by a light microscopy (Nikon type E600, Japan) as described previously (*7*). The size of AOBs was determined by measurement of laser light scattering at a 90° angle with N4-submicrometer particle size analyzer (Beckman Coulter, USA). Each data point represents the mean ± standard deviation (SD) from three independent measurements. Furthermore, AOBs were also analyzed using transmission electron microscopy (Jeol JEM-1400, Japan). One drop of RGD-tagged AOB suspension was placed on a 400 mesh copper grid coated with carbon. After deposition for 2 min, the grid was tapped with a filter paper to remove surface water before negative staining with uranyl acetate solution. Meanwhile, the stability of AOBs was determined by the turbidity test according to the previous method (*7*). In brief, 1 mL of AOB solution was placed in a cuvette. Covered with parafilm, the cuvette containing AOBs was kept at the indicated condition. The absorbance (A) of the suspension in the lower portion of the cuvette was measured at 600 nm with spectrophotometer (Beckmen DU 530, USA). The absorbance read at the beginning (A_0) and time intervals (A) was used for calculation of the relative turbidity.

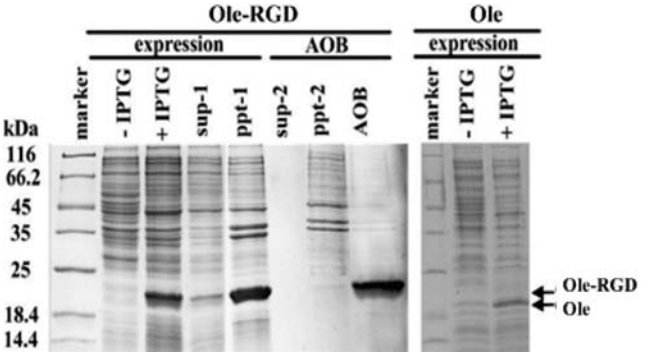

Figure 1. SDS−PAGE analyses of Ole-RGD overproduction in *E. coli* strain. As described, recombinant *E. coli* strains were grown in shake flasks and induced by IPTG for protein production. At the end of culturing, bacterial cells were harvested and processed for SDS−PAGE analyses. Total proteins from induced (+IPTG) and uninduced (−IPTG) strain BL21-OleTR (left panel) and BL21-Ole (right panel) were resolved in SDS−PAGE. Moreover, the total protein of strain BL21-Ole was fractioned into the soluble part (sup-1) and insoluble part (ppt-1). Ole-RGD in the insoluble fraction was then recovered and mixed with olive oil and PL. After sonication, AOBs floating on the top with two other fractions, the supernatant (sup-2) and precipitate (ppt-2), were obtained by centrifugation at 10000*g* for 15 min. AOBs were isolated and heated to release the protein (AOB) as analyzed by SDS−PAGE.

Cell Culture. Human tumor cell lines, MDA-MB-231, SKOV3, SKBR3, and MCF7, were maintained in DEME/F12 medium (HyClone Lab., USA) supplemented with 10% fetal bovine serum (FBS) and cultured at 37 °C in a humidified atmosphere of 5% CO_2 incubator. The culture medium was changed every 2 days until cell confluence reached 80%. Cell concentration was counted by hemocytometer, and cells were resuspended and seeded into a 24-well plate to reach 1×10^5 cells per well.

Fluorescence Microscopy, Confocal Microscopy, and Flow Cytometry. To react with AOBs, tumor cells were washed with a phosphate buffer solution (PBS) of pH 7.4 and fixed with 3.7% formaldehyde at room temperature for 15 min. Followed by washing with PBS, AOBs were added to the cells for interaction at 37 °C for 30 min. Subsequently, cells were washed with PBS containing 0.01% Tween-20 once and PBS twice. A blocking solution, consisting of 3% FBS albumin in PBS, was added to cells at room temperature for 1 h. Finally, anti-integrin $\alpha_v\beta_3$ antibody (Santa Cruz Biotech., USA) of 200-fold dilution was added to react at room temperature for 1 h. After rinsing three times with PBS, anti-mouse IgG-TRIAC (Jackson ImmunoResearch Lab., USA) of 500-fold dilution was applied for reaction and washed with PBS to remove the unbound secondary antibody. In addition, cell nuclei were stained by diamidino-2-phenylindole (DAPI) of 15,000-fold dilution and washed with PBS. The cells were visualized with fluorescence microscopy (Olympus IX71, Japan) and confocol microscopy (Leica TCS SP2, Germany).

Alternatively, tumor cells were seeded into a 6-well plate (1×10^5 cells per well) and grown to 80% confluence. After incubation with AOBs, cells were washed twice with PBS. Followed by trypsinization, cells were harvested by centrifugation and resuspended in PBS. Analysis of internalized AOBs was conducted using a FACScanto flow cytometer system (Becton Dickinson, USA).

RESULTS

Reconstitution of Ole-RGD-Based AOBs. To examine the production of Ole-RGD, *E. coli* strain BL21-OleTR and BL21-Ole were cultivated and induced by IPTG. As analyzed by SDS−PAGE (**Figure 1**), Ole-RGD was overexpressed in strain BL21-OleTR in response to IPTG and could be found mainly in the insoluble fraction of cell lysate (ppt-1). Insoluble Ole-RGD was then recovered to reconstitute AOBs. Followed by centrifugation,

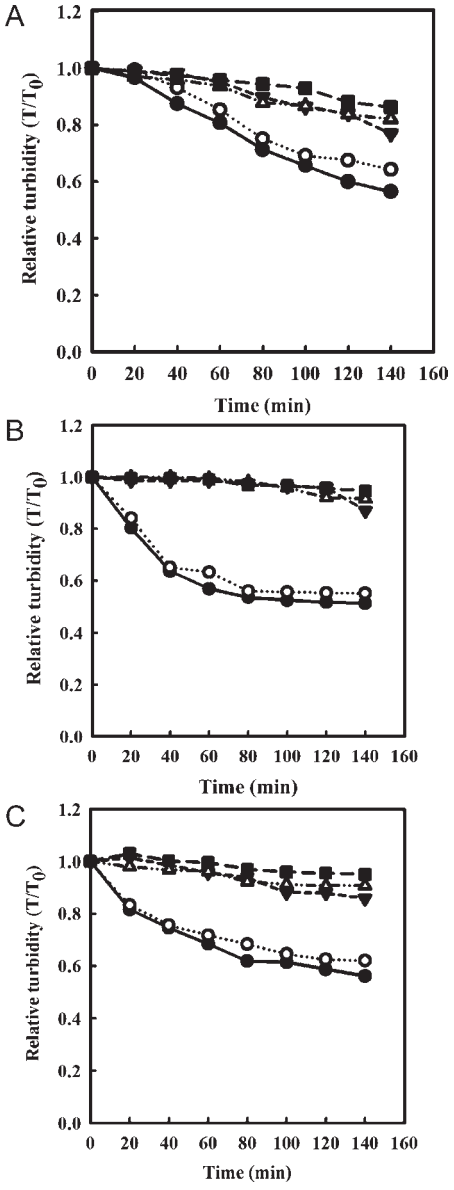

Figure 2. Stability of AOBs reconstituted at various conditions. The stability of AOBs prepared at various conditions was examined by the turbidity test at room temperature as described. (**A**) AOBs were prepared with various types of oils at 4 °C and pH 7.5. Symbols: sesame oil (■); soybean oil (△); olive oil (▼); peanut oil (○); mineral oil (●). (**B**) Preparation of AOBs was carried out by using various Oil/Ole ratios at 4 °C and pH 7.5. Symbols: the weight ratio at 10:1 (●); the weight ratio at 2:1 (○); the weight ratio at 1:1 (▼); the weight ratio at 1:5 (△); the weight ratio at 1:10 (■). (**C**) With Oil/Ole at 1:1, AOBs were reconstituted at 4 °C and various pH. Symbols: pH 6.5 (●); pH 7.0 (○); pH 7.5 (▼); pH 8.0 (△); pH 9.0 (■).

it resulted in the formation of AOBs floating on the top of supernatant (sup-2) with few proteins left in the cell pellet (ppt-2). Isolated AOBs were heated and readily disintegrated to liberate incorporated proteins from which Ole-RGD was identified as the main protein (AOB). Its molecular weight was estimated to reach 21 kDa as expected. This result indicates the strong association of Ole-RGD with oils. Similarly, recombinant Ole overexpressed in strain BL21-Ole was present mostly in the form of inclusion bodies upon IPTG induction.

Condition for Reconstitution of Ole-RGD-Based AOBs. The conditions for reconstitution of Ole-RGD-based AOBs were investigated in a systematic way. First, various types of plant oils were examined for their effect on the stability of AOBs. This was carried out by mixing Ole-RGD and PL with various plant oils. In general, it led to relatively stable formation of AOBs as prepared with sesame oil, soybean oil or olive oil (**Figure 2A**).

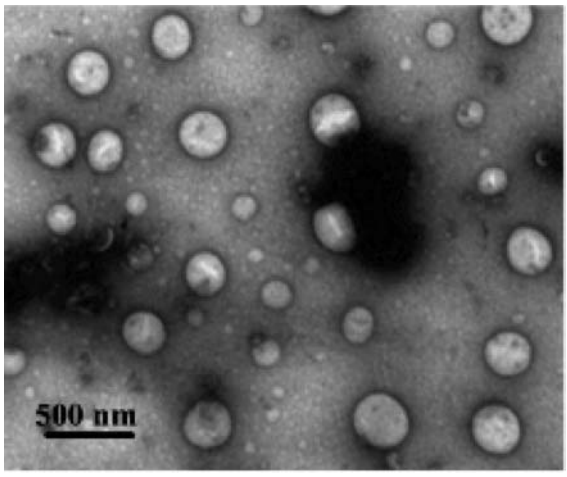

Figure 3. Morphology examination of the RGD-tagged AOBs by TEM. As described, RGD-tagged AOBs were constituted and examined by TEM.

Table 1. Particle Size of RGD-Based AOBs Prepared at Various Values of Oil/Ole and pH

A		B	
Oil/Ole (w/w)	mean particle size (nm)	pH	mean particle size (nm)
10:1	1173.1 ± 24.1	6.5	787.7 ± 36.6
2:1	783.1 ± 16.8	7.0	472.5 ± 24.3
1:1	412.5 ± 23.4	7.5	339.3 ± 34.0
1:5	200.9 ± 47.7	8.0	159.6 ± 25.8
1:10	42.9 ± 4.3	9.0	77.9 ± 3.3

Moreover, AOBs were prepared with the various weight ratios of oil to Ole-RGD (Oil/Ole). Their size was found to decrease with lower Oil/Ole (**Table 1**). As prepared with lower Oil/Ole, AOBs exhibited higher stability (**Figure 2B**) and had size ranging between 40 and 410 nm (**Table 1**). Finally, AOBs were constituted with olive oil at various pH. Owing to the instability of AOBs in acidic conditions (*7*), the condition pH > 6.5 was chosen for study. As shown in **Figure 2C**, AOBs formed at pH exceeding 7.0 were more stable. The mean distribution of their size was within the range 80−340 nm (**Table 1**).

Selective Internalization of RGD-Tagged AOBs into Cells. For the rest of the experiments, the conditions for preparation of AOBs were chosen as follows: the weight ratio of olive oil to Ole at 1:1 and pH 7.5. To investigate their biological function, the Ole-RGD-based AOBs were entrapped with the hydrophobic fluorescent dye. It was found that the stability of AOBs remained unaffected with the entrapment of 1 μg/mL fluorescent dye. In addition, morphology examination of AOBs was further conducted using transmission electron microscopy (TEM). The result revealed the mean particle size ranging between 200 and 300 nm (**Figure 3**), approximately in agreement with that (300−400 nm) as measured by laser light scattering (**Table 1**). Note that the size determined by TEM is the diameter of objects at the dehydrated state, while that by laser light scattering is the hydrodynamic diameter (hydrated state). This would account for the measurement discrepancy in particle sizes by these two methods.

Subsequently, these fluorescent AOBs were coincubated with various cell types that were prefixed. As visualized by fluorescence microscopy (**Figure 4A**), Ole-RGD-based AOBs were able to adhere to $\alpha_v\beta_3$ integrin-positive cells (e.g., SKOV3) instead of

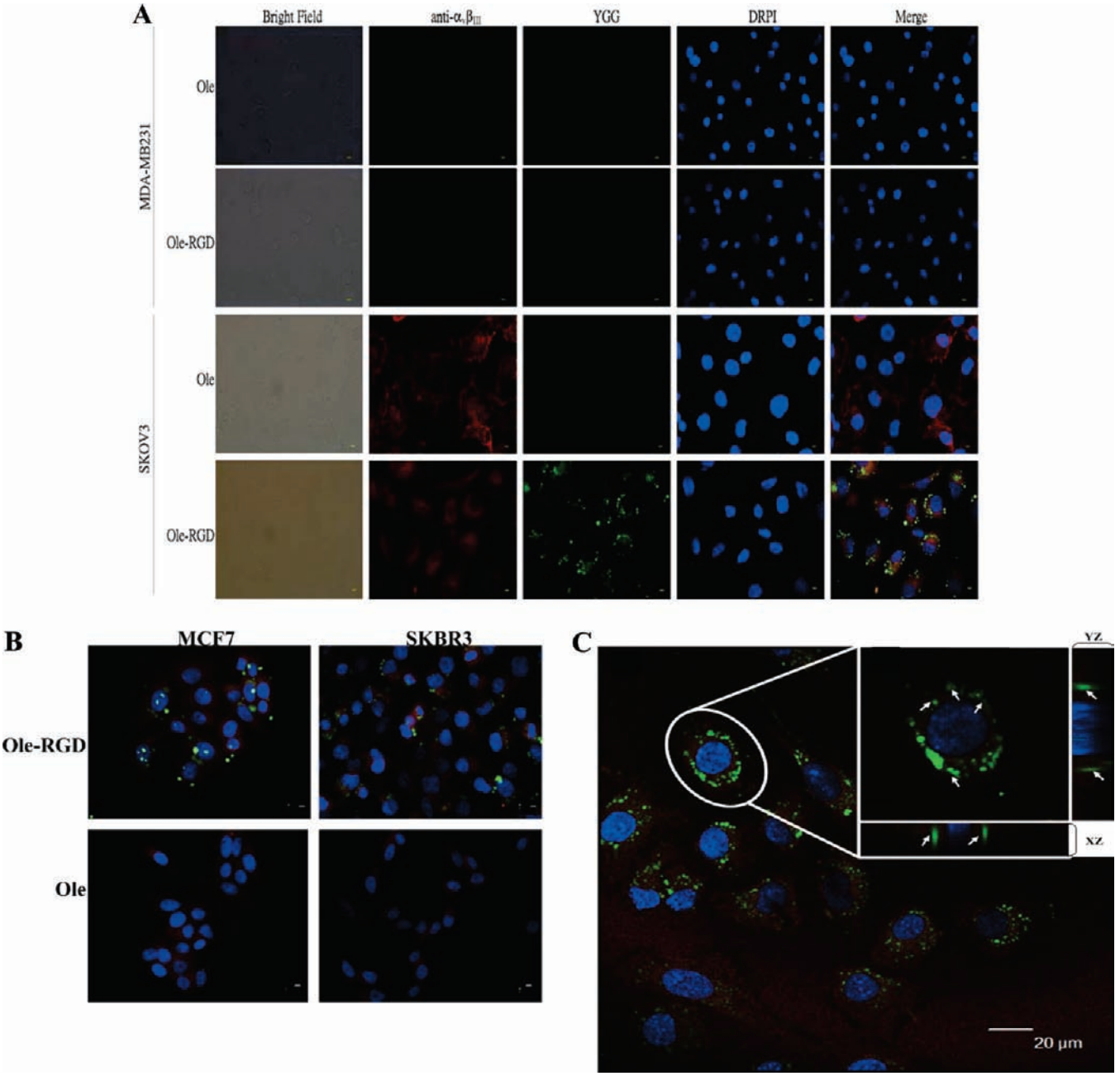

Figure 4. Targeting tumor cells by AOBs with fluorescence and confocal microscopy. AOBs were prepared with an equal weight of Ole-RGD (or Ole) vs olive oil and 1 μg/mL fluorescent dye at 4 °C and pH 7.5. Subsequently, AOBs resuspended in PBS were added to 1×10^5 cells with the final concentration of 25 ng/mL. (**A**) Tumor cells, $\alpha_v\beta_3$ integrin-negative MDA-MB-231 cell (upper) and $\alpha_v\beta_3$ integrin-positive SKOV3 cell (bottom), were fixed with paraformaldehyde on a glass slide. Followed by washing with PBS buffer solution, the fixed cells were coincubated with fluorescent AOBs (green) consisting of Ole or Ole-RGD. After 30 min, cells were extensively washed with PBS buffer 3 times. For further observation by fluorescence microscopy, cell nuclei (blue) were stained by DAPI and the $\alpha_v\beta_3$ integrin receptor (red) was stained with anti-$\alpha_v\beta_3$ integrin antibody. The image was individually taken and then merged as shown on the right. (**B**) Similarly, two $\alpha_v\beta_3$ integrin-positive cells, SKBR3 and MCF7, were grown in 24-well plates. Without prefixing, cells were coincubated with fluorescent AOBs (green) that were made from either Ole or Ole-RGD for 120 min. After washing with PBS buffer, cells were taken for analysis using fluorescence microscopy. (**C**) Coincubation of live $\alpha_v\beta_3$ integrin-stained SKOV3 (red) with RGD-tagged AOBs (green) was carried out and analyzed by confocal laser scanning microscopy (CLSM). Each panel represents a section from the stack on the *z* axis which is appropriately chosen for clear visualization. Two three-dimensional reconstruction sections perpendicular to the plane of the monolayer and parallel to the *x* or *y* axis are shown below (*x*−*z* section) and to the right (*y*−*z* section) of the inset. A part of internalized AOBs is indicated by white arrows.

$\alpha_v\beta_3$ integrin-negative cells (e.g., MDA-MB-231). Moreover, the controls (AOBs free of RGD) were not associated with any cells.

When incubated with $\alpha_v\beta_3$ integrin-positive tumor cells without prefixing, RGD-tagged AOBs became internalized and clustered in the cytoplasmic space of cells (**Figure 4B**). This was further confirmed by confocal microscopy (**Figure 4C**). Taken together, these results indicate the successful presentation of the RGD motif on the AOBs' surface, thereby leading to the selective internalization of AOBs by $\alpha_v\beta_3$ integrin-positive cells.

Internalization Efficiency of RGD-Tagged AOBs. The internalization efficiency of RGD-tagged AOBs by $\alpha_v\beta_3$ integrin-positive cells was evaluated on the basis of two factors, including the incubation time and the incubation dose. Therefore, by incubation with 25 ng/mL AOBs for various periods of time, cells were

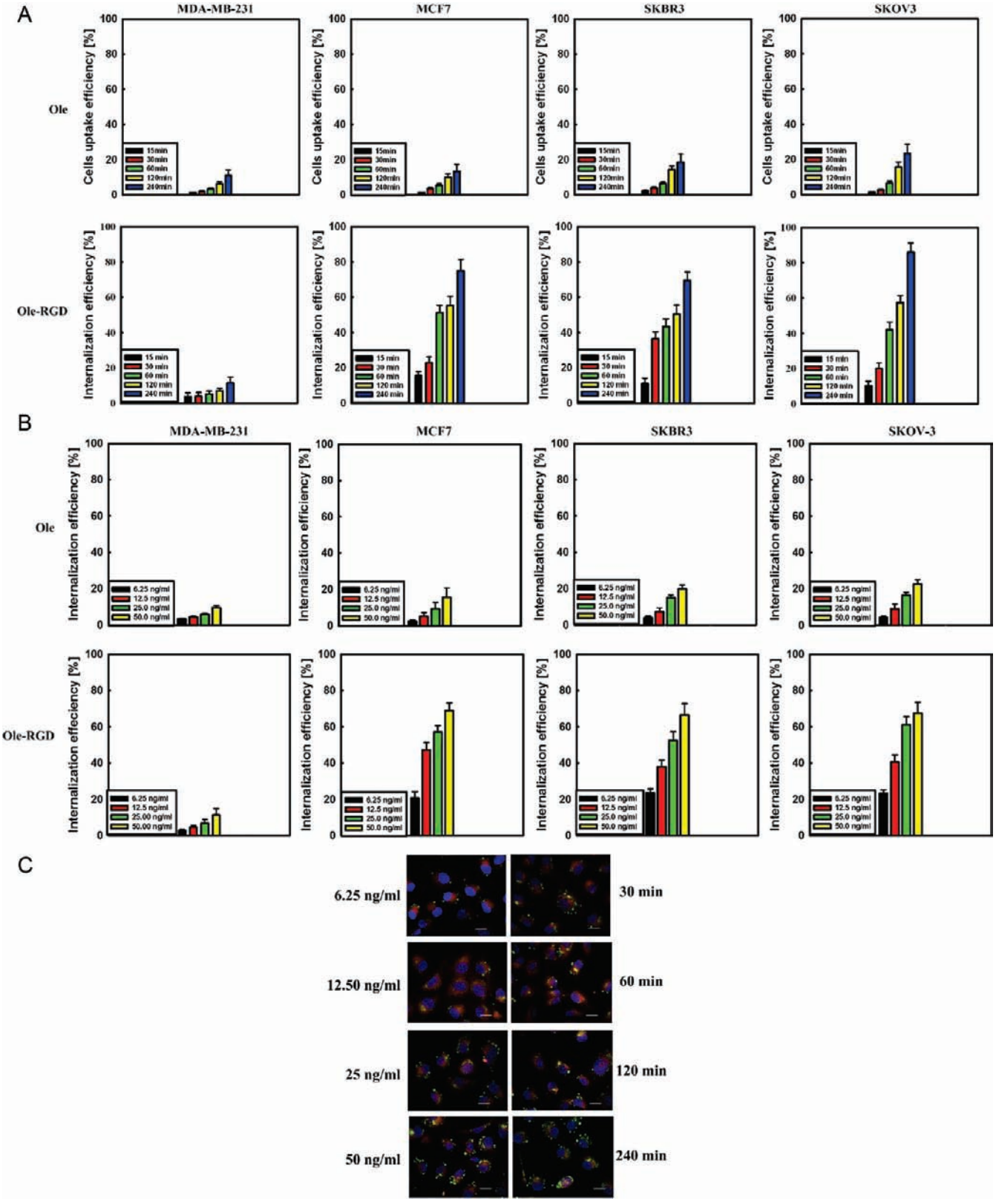

Figure 5. Internalization efficiency of RGD-tagged AOBs by flow cytometry and confocal microscopy. AOBs were prepared and incubated with tumor cells without prefixing as described in **Figure 4**. Cell lines chosen for test included MDA-MB-231 (control) and three $\alpha_v\beta_3$ integrin-positive cells, such as MCF7, SKOV3, and SKBR3. At the end of experiments, cells were collected for further analyses. (**A**) The effect of incubation time on internalization efficiency. Coincubation of tumor cells with 25 ng/mL AOBs was carried out for various time and processed for analysis by flow cytometry. (**B**) The effect of incubation dose on internalization efficiency. Tumor cells were incubated with various concentrations of AOBs for 120 min and then processed for analysis by flow cytometry. All experiments were conducted in triplicate. Symbols: Ole, Ole-based AOBs; Ole-RGD, Ole-RGD-based AOBs. (**C**) Analysis of tumor cells interacting with AOBs by confocal microscopy. Interaction of SKOV3 cells with RGD-based AOBs was analyzed by CLSM at various doses (left panel) and incubation time (right panel).

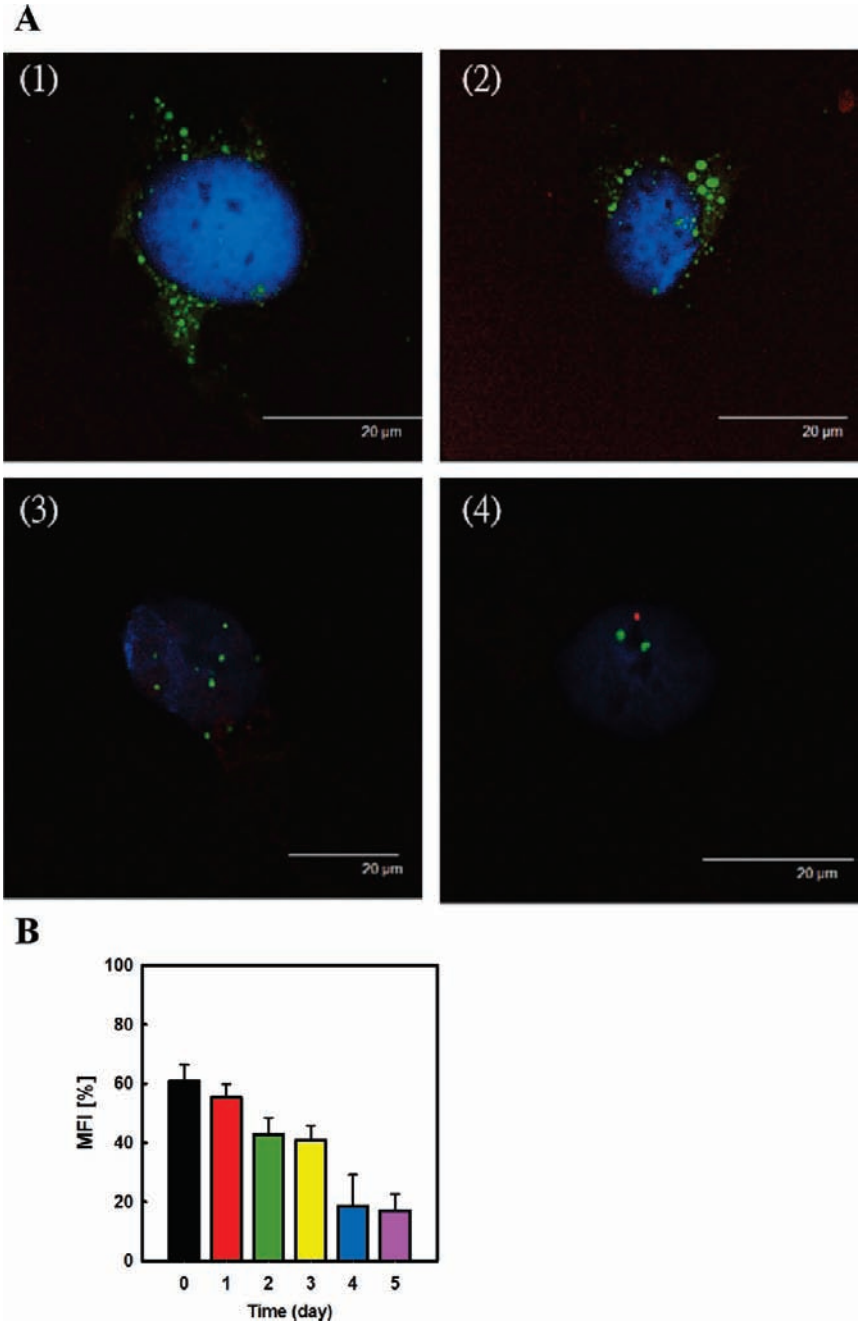

Figure 6. Release and decay of the fluorescence dye carried by AOBs. Refer to **Figure 4**, coincubation of live SKOV3 cells with RGD-based AOBs was carried out in a similar way. The fate of internalized AOBs in the cells was then tracked along the time course. (**A**) At the end of experiment, cells were taken for observation by fluorescence microscopy on (**1**) day 1, (**2**) day 2, (**3**) day 3, and (**4**) day 4. (**B**) Meanwhile, cells were processed for analysis by flow cytometry. The mean fluorescence intensity (MFI) was measured for each day as indicated. Three independent measurements were performed.

collected and processed for analysis by flow cytometry. In general, the percentage of cells internalized by RGD-tagged AOBs increased with increasing incubation time. It reached approximately 80% for $\alpha_v\beta_3$ integrin-positive cells (e.g., MCF7, SKOV3, and SKBR3) when incubation time persisted for 240 min (**Figure 5A**). Among tumor cells examined here, SKOV3 exhibited the highest efficiency in uptake of RGD-based AOBs. Alternatively, tumor cells were incubated with various doses of AOBs for 120 min. The percentage of cells internalized by RGD-tagged AOBs was dependent on the AOB concentration (**Figure 5B**). Within the range of 25−50 ng/mL AOBs, the internalization efficiency could reach the maximum (roughly 80%) for $\alpha_v\beta_3$ integrin-positive cells. Further examination by CLSM confirmed the presence of RGD-tagged AOBs within the cells (**Figure 5C**).

Release of the Carried Fluorescent Dye. A good delivery carrier is featured with the capability to liberate the cargo entities that it carries upon entry into target cells. Therefore, we were prompted to investigate the controlled release feature of AOBs. SKOV3 cells were then incubated with 25 ng/mL RGD-tagged AOBs for 120 min. Subsequently, cells were collected and subjected to further analysis by fluorescence microscopy and flow cytometry along the time course. As depicted in **Figure 6A**, fluorescent spots within the cells started to decay as time elapsed. After 4 days, the fluorescent signal was marginally detected. This observation was correlated with the decay profile of fluorescence intensity analyzed by flow cytometry (**Figure 6B**). It implies that the hydrophobic dye released from AOBs decomposes within the cells.

DISCUSSION

Targeted therapy of tumor vasculature has been by far considered as the most powerful means for treatment of cancers. The essence of these approaches strongly relies on the specific interaction of the biomarker presented on the tumor cells with the binding ligand. One well-known example is the selective recognition of the $\alpha_v\beta_3$ integrin, mainly expressed on angiogenic endothelial cells, by the RGD-based peptide (*24*). Accordingly, many delivery vehicles conjugated with the RGD-containing peptide have been developed to achieve targeted drug delivery and tumor imaging (*21*). AOBs are oil droplets with high stability. In particular, their hydrophobic nature and excellent capability to display peptides make them appealing as a drug delivery carrier. To this end, our first step toward this goal was taken to present the RGD-cored peptide onto AOBs' surface. This was simply conducted following the procedure outlined in **Figure 6**. The first step was to recover insoluble Ole-RGD overexpressed in *E. coli*. Followed by mixing Ole-RGD with oils and the fluorescent dye, the mixture was subjected to sonication. After a brief centrifugation, AOBs acting like a milky "scum" were formed on the top. Recovery of the scum in the buffer solution gave rise to the RGD-tagged AOBs that were entrapped with the fluorescent dye.

The stability of RGD-tagged AOBs was correlated with their size. On the whole, stable AOBs had a size in the range 100−400 nm (**Table 1**) and the size could be tailored by manipulating three factors, such as oil type, Oil/Ole, and pH (**Figure 2A**−**C**). Further illustration showed that AOBs equipped with RGD were able to selectively penetrate $\alpha_v\beta_3$ integrin-positive cells (**Figures 4B** and **4C**). Without RGD, AOBs became noninvasive. Indeed, two extruded peptide arms of Ole confer on AOBs a negative surface charge (*4*), and this would prevent the undesired interaction with the nontarget cells (*25*). Apparently, this unique feature of AOBs makes them advantageous to serve as a delivery vehicle. It has been reported that the amino acid residues flanking RGD could impart a profound effect on the conformational feature of RGD, which in turn affects its affinity and specificity (*26*). Therefore, the present result clearly indicates the feasibility of Ole for functional processing of RGD on AOBs' surface. In addition, the efficiency of RGD-mediated internalization of AOBs into $\alpha_v\beta_3$ integrin-positive cells could account for as high as 80%. This high uptake rate suggests the presence of multivalent RGD on AOBs according to the previous report (*27*).

The major pathway implemented by delivery carriers to enter nonphagocytic cells is known as the zipper mechanism (*28*). It relies on the direct contact between the binding ligand of the carrier and cellular receptors. As a result of close attachment, local cytoskeletal rearrangement occurs, which in turn induces the uptake of the delivery carrier in an enclosed vacuole. The RGD-mediated endocytosis is well documented and proceeds in a similar way (*29*). This is probably reflected by the observation of heterogeneous distribution of internalized AOBs in $\alpha_v\beta_3$ integrin-positive cells (**Figure 4B**). Indeed, AOBs tend to aggregate in an acidic condition, ultimately resulting in their disintegration (*7*). This leads to the control-and-release feature of AOBs upon entry into the acidic endosomes (*30*, *31*). Therefore, the RGD-triggered endocytosis of AOBs allows liberation of the carried cargo entity (e.g., hydrophobic fluorescence dye) as depicted in **Figure 6**.

In summary, AOBs linked with binding ligands and entrapped with waster-insoluble agents can be simply and reproducibly made in a single step (**Figure 7**). Particularly, they have superior cellular targeting and internalization ability, tunable size, favorable surface charge, and acid-triggered release property. The usefulness of AOBs for targeted drug delivery is currently under investigation, and the result is encouraging (*32*). It is anticipated that the advance of this proposed approach in the near future shall open a new avenue for targeted delivery of therapeutic entities.

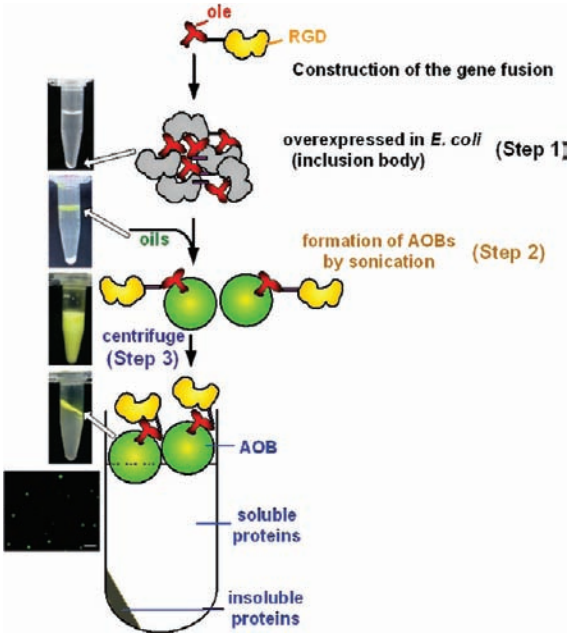

Figure 7. Schematic illustration of the protocol for preparing fluorescent RGD-based AOBs. In the first step, the fusion gene consisting of Ole and the RGD motif was constructed and expressed in *E. coli*. Bacterial cells were disrupted and centrifuged to precipitate Ole-RGD on the bottom of the sample tube (indicated by an arrow). Second, the mixture containing recovered Ole-RGD, oils, and the fluorescent dye was subjected to sonication, resulting in the opaque solution with suspensions. Finally, centrifugation was applied to separate the scum AOBs on the top of the sample tube (indicated by an arrow). Isolated AOBs were dispersed in the solution and visualized by fluorescence microscopy.

ACKNOWLEDGMENT

We would like to acknowledge Instrument Center of R&D Office at China Medical University for technical assistance.

LITERATURE CITED

(1) Huang, A. H. Oleosins and oil bodies in seeds and other organs. *Plant Physiol.* **1996**, *110*, 1055−1061.
(2) Napier, J. A.; Stobart, A. K.; Shewry, P. R. The structure and biogenesis of plant oil bodies: the role of the ER membrane and the oleosin class of proteins. *Plant Mol. Biol.* **1996**, *31*, 945−956.
(3) Frandsen, G. I.; Mundy, J.; Tzen, J. T. C. Oil bodies and their associated proteins, oleosin and caleosin. *Plant Physiol.* **2001**, *112*, 301−307.
(4) Tai, S. S. K.; Chen, M. C. M.; Peng, C. C.; Tzen, J. T. C. Gene family of oleosin isoforms in sesame seed oil bodies. *Biosci. Biotechnol. Biochem.* **2002**, *66*, 2146−2153.
(5) Tzen, J. T. C.; Lie, G. C.; Huang, A. H. Characterization of the charged components and their topology on the surface of plant seed oil bodies. *J. Biol. Chem.* **1992**, *267*, 15626−15634.
(6) Tzen, J. T. C.; Chuang, R. L.; Chen, J. C.; Wu, L. S. Coexistence of both oleosin isoforms on the surface of seed oil bodies and their individual stabilization to the organelles. *J. Biochem.* **1998**, *123*, 318−323.
(7) Peng, C. C.; Lin, I. P.; Lin, C. K.; Tzen, J. T. C. Size and stability of reconstituted sesame oil bodies. *Biotechnol. Prog.* **2003**, *19*, 1623−1626.
(8) Tzen, J. T. C.; Huang, A. H. Surface structure and properties of plant seed oil bodies. *J. Cell Biol.* **1992**, *117*, 327−335.

(9) Peng, C. C.; Chen, J. C. F.; Shyu, D. J. H.; Chen, M. J.; Tzen, J. T. C. A system for purification of recombinant proteins in *Escherichia coli* via artificial oil bodies constituted with their oleosin-fused polypeptides. *J. Biotechnol.* **2004**, *111*, 51−57.

(10) Chiang, C. J.; Chen, H. C.; Chao, Y. P.; Tzen, J. T. C. Efficient system of artificial oil bodies for functional expression and purification of recombinant nattokinase in *Escherichia coli*. *J. Agric. Food Chem.* **2005**, *53*, 4799−4804.

(11) Chiang, C. J.; Chen, H. C.; Chao, Y. P.; Tzen, J. T. C. One-step purification of insoluble hydantoinase overproduced in *Escherichia coli*. *Protein Expression Purif.* **2007**, *52*, 14−18.

(12) Chiang, C. J.; Chen, H. C.; Kuo, H. F.; Chao, Y. P.; Tzen, J., T. C. A simple and effective method to prepare immobilized enzymes using artificial oil bodies. *Enzyme Microb. Technol.* **2006**, *39*, 1152−1158.

(13) Hou, R. C.; Lin, M. Y.; Wang, M. M.; Tzen, J. T. C. Increase of viability of entrapped cells of *Lactobacillus delbrueckii* ssp. *bulgaricus* in artificial sesame oil emulsions. *J. Dairy Sci.* **2003**, *86*, 424−428.

(14) Lipinski, C. A.; Lombardo., F.; Dominy, B. W.; Feeney, P. J. Experimental and computational approaches to estimate solubility and permeability in drug discovery and development settings. *Adv. Drug Delivery Rev.* **2000**, *46*, 3−36.

(15) Fernandez, A. M.; Van derpoorten, K.; Dasnois, L.; Lebtahi, K.; Dubois, V.; Lobl, T. J.; Gangwar, S.; Oliyai, C.; Lewis, E. R.; Shochat, D.; Trouet, A. N-Succinyl-(β-alanyl-l-leucyl-l-alanyl-l-leucyl)doxorubicin: an extracellularly tumor-activated prodrug devoid of intravenous acute toxicity. *J. Med. Chem.* **2001**, *44*, 3750−3753.

(16) Andresena, T. L.; Jensenb, S. S.; Jørgensen, K. Advanced strategies in liposomal cancer therapy: problems and prospects of active and tumor specific drug release. *Prog. Lipid Res.* **2005**, *44*, 68−97.

(17) Zhang, L.; Chan, J. M.; Gu, F. X.; Rhee, J. W.; Wang, A. Z.; Radovic-Moreno, A. F.; Alexis, F.; Langer, R.; Farokhzad, O. C. Self-assembled lipid-polymer hybrid nanoparticles: a robust drug delivery platform. *ACS Nano* **2008**, *2*, 1696−1702.

(18) Torchilin, V. P. Lipid-core micelles for targeted drug delivery. *Curr. Drug Delivery* **2005**, *2*, 319−327.

(19) Cohen, S. N.; Bernstein, H. *Microparticulate systems for the delivery of proteins and vaccines*; Marcel Dekker: New York, 1996.

(20) Torchilin, V. P. Micellar nanocarrier: pharmaceutical perspectives. *Pharm. Res.* **2007**, *24*, 1−16.

(21) Temminga, K.; Schiffelersc, R. M.; Molemad, G.; Kok, R. J. RGD-based strategies for selective delivery of therapeutics and imaging agents to the tumour vasculature. *Drug Resist. Updates* **2005**, *8*, 381−402.

(22) Miller, J. H. *Experiments in molecular genetics*; Cold Spring Harbor Laboratory: Cold Spring Harbor, NY, 1972.

(23) Chiang, C. J.; Chern, J. T.; Wang, J. Y.; Chao, Y. P. Facile immobilization of evolved *Agrobacterium radiobacter* carbamoylase with high thermal and oxidative stability. *J. Agric. Food Chem.* **2008**, *56*, 6348−6354.

(24) Martin, M. E.; Rice, K. G. Peptide-guided gene delivery. *AAPS J.* **2007**, *9*, 18−29.

(25) Suh, W.; Han, S. O.; Yu, L.; Kim, S. W. An angiogenic, endothelial-cell-targeted polymeric gene carrier. *Mol. Ther.* **2002**, *6*, 664−672.

(26) Pierschbacher, M. D.; Ruoslahti, E. Influence of stereochemistry of the sequnece Arg-Gly-Asp-Xaa on binding specificity in cell adhesion. *J. Biol. Chem.* **1987**, *262*, 17294−17298.

(27) Boturyn, D.; Coll, J. L.; Garanger, E.; Favrot, M. C.; Dumy, P. Template assembled cyclopeptides as multimeric system for integrin targeting and endocytosis. *J. Am. Chem. Soc.* **2004**, *126*, 5730−5739.

(28) Vassaux, G.; Nitcheu, J.; Jezzard, S.; Lemoine, N. R. Bacterial gene therapy strategies. *J. Pathol.* **2006**, *208*, 290−298.

(29) Schraa, A. J.; Kokb, R. J.; Berendsena, A. D.; Moorlaga, H. E.; Bosb, E. J.; Meijerb, D. K. F.; de Leija, L. F. M. H.; Molema, G. Endothelial cells internalize and degrade RGD-modified proteins developed for tumor vasculature targeting. *J. Controlled Release* **2002**, *83*, 241−251.

(30) Ohkuma, S.; Poole, B. Fluorescence probe measurement of the intralysosomal pH in living cells and the perturbation of pH by various agents. *Proc. Natl. Acad. Sci. U.S.A.* **1978**, *75*, 3327−3331.

(31) Yamashiro, D. J.; Fluss, S. R.; Maxfield, F. R. Acidification of endocytic vesicles by an ATP-dependent proton pump. *J. Cell Biol.* **1983**, *97*, 929−934.

(32) Chiang, C. J.; Chao, Y. P. Personal communication.

Received for review July 28, 2010. Revised manuscript received September 23, 2010. Accepted October 4, 2010. This work was supported by Taiwan National Science Council (NSC 99-2313-B-039-003-My3), China Medical University (CMU 97-282, CMU98-N2-22, and CMU98-C-11), and Feng Chia University (08G27501).